Fast Electro-Thermal Simulation of Short-Circuit Tests

C. Abomailek[1], J.-R. Riba[1*], F. Capelli[1], and M. Moreno-Eguilaz[2].

[1] Electrical Engineering Department, Universitat Politècnica de Catalunya, 08222 Terrassa, Spain
[2] Electronics Engineering Department, Universitat Politècnica de Catalunya, 08222 Terrassa, Spain
[*] Corresponding author: riba@ee.upc.edu

Abstract— Low- and medium-voltage connectors are designed for a service life of more than 30 years, during which they have to withstand extreme conditions, so it is primordial ensuring their thermal performance. Mandatory standardized short-circuit tests are required to homologate electrical connectors which are conducted in singular and scarce laboratories, so it is essential to dispose of fast and accurate simulation tools to predict the thermal performance of the equipment during the design stage. This paper focuses on the application of a fast and accurate simulation method to reproduce the transient thermal behavior and to estimate the transient temperature rise and the subsequent cooling of power connectors during short-circuits. To minimize the computational burden, this paper proposes a fast FDM (finite difference method) approach, based on one-dimensional reduction of the analyzed geometry. To improve accuracy, key three-dimensional information is retained, such as the convective coefficients, the incremental resistance or the cross-section of each node. Results attained by means of the proposed method are validated against experimental results conducted in a high-current laboratory, thus corroborating the usefulness and accuracy of the proposed method. The methodology exposed in this paper can be applied to many other hardware for power lines and substations.

1. INTRODUCTION

Power transmission systems are expanding due to the increasing consumption of electrical power worldwide [1]. Short-circuit fault current levels in power systems are raising [2], which can produce severe faults due to both the unusual thermal and mechanical stress the components have to withstand, thus increasing the risk of power system failure [3]. Therefore, it is essential ensuring that fault currents do not compromise the safety limits of the involved electrical equipment. It is an accepted fact that the service life of the involved equipment can be improved by reducing the temperature achieved during the short-circuit phenomenon [4]. The development of accurate methods to predict the temperature rise during short-circuit conditions is of paramount importance since it can significantly influence the optimum design process of the involved equipment [5]. Short-circuit analysis is important since it allows determining the rating of power apparatus [6]. Power connectors and many other power devices must be tested to pass the mandatory short-time withstand current and peak withstand current tests to ensure to withstand the thermal conditions due to short-circuits, which are defined in different international standards [7–9].

This paper analyses the thermal behaviour of medium voltage connectors during short-circuit faults. To this end a fast and accurate simulation model based on dimensional reduction and applying a FDM (finite

difference method) approach is presented to predict the transient thermal behaviour of low- and medium-voltage connectors during the fault condition.

Low-, medium- and high-voltage connectors must be tested according to the international standards, which comprise, among others, the short-time withstand current test and peak withstand current test. Experimental short-circuit tests must be carried out in singular laboratories, with huge electrical power requirements. Due to the singularity and scarcity of such laboratories, connectors manufacturers often have to face long waiting times before tests are made, thus resulting in cost increases and manufacturing delays. Due to the high costs associated to short-circuit tests [10] and to ensure that the analysed power connectors satisfy the thermal requirements settled by the international standards, the development of fast, accurate and reliable software tools for simulating such tests are thus highly appealing. Such simulations must be able to replicate the real thermal and electromagnetic behaviour of the device under test in a fast and economical way.

The analysis of the thermal performance of electrical devices under harsh short circuit conditions is of great interest to ensure that such devices can withstand these harsh conditions without experiencing an irreversible damage or a perceptible lifespan reduction which can jeopardize the efficient and safe operation. To this end different FEM analysis for air circuit breakers [11], superconducting cables [1], electrical generators [5], bus bar systems [12], plug-in connectors [13] or power connectors [14] under short-circuit condition are found in the recent technical literature. However, most of the abovementioned references are based on three-dimensional FEM simulations, which present several weaknesses, including the use of costly software licenses, or an intensive dedication of a skilled engineer to conduct the time-consuming tasks associated for arranging the 3D geometry, generating the 3D meshes, or settling the boundary conditions among others as well as the high computational burden associated. Consequently, the use of accurate approaches based on model reduction [15, 16], model-order reduction [17] or approaches combining thermal lumped-element networks with electrical models [19] are appealing because they can overcome the aforementioned shortcomings of FEM simulations.

This work proposes a fast one-dimensional simulation method based on nodal equations and the application of the finite difference method (FDM) for estimating the temperature rise in power conductors during short-circuit tests as well as the cooling phase once the short-circuit current has been cleared. Although the proposed model deals with the inherent singularities of short-circuit tests and bimetallic connectors for low- and medium-voltage applications, it is based on the approach presented in [18] which deals with bolted aluminum substation connectors for high-voltage applications. The analysis of the short-circuit behavior presents different particularities and challenges with respect to the study of the temperature

rise test presented in [18], such as the short duration in which the adiabatic approximation applies during the heating phase, the transient nature of the current waveform during the initial stage of the short-circuit, or the wider and sudden temperature rise because of the extreme thermal stress during the short-circuit condition. The one-dimensional model discretizes the analyzed geometry in several small elements or nodes. This approach allows increasing accuracy and a great reduction of the computational burden. Each nodal element retains some information about the three-dimensional geometry of the analyzed device, being this information applied to calculate the convective coefficient and the incremental resistance of each node at every time-step during the simulation.

2. THE TESTED CONNECTORS

This section describes the bimetallic copper-aluminum YAT120AM130CP compression connectors for low- and medium-voltage applications analyzed in this work, from the catalogue of SBI Connectors, which are shown in Fig. 1. Aluminum material is type EN AW-1050A as per the EN 573-3:2014 standard [20], whereas copper material is Cu-ETP as per the EN 13601:2014 standard [21]. To maximize the contact between the conductor and the barrel of the connector, the entire contact surface has been compressed by using a 69 MPa BURNDI EP-1HP crimping tool.

Fig. 1. YAT120AM130CP connectors. a) Before compression. b) After compression. c) CAD drawing including the bolting elements.

3. THE SHORT-CIRCUIT TEST

Power connectors are often designed to meet the requirements of the IEC 61238-1 international standard [22], which is applicable for mechanical and compression connectors designed for aluminium or copper conductors of power cable with rated voltages up to 30 kV. The IEC 61238-1 standard requires a stable resistance of the connection, the temperature of the connector remaining below that of the reference conductor, and an adequate mechanical strength of the connector. According to this standard, due their nature, Class A connectors, that is, those intended for the majority of applications including industrial networks or electricity distribution, must be able to withstand short-circuits of relatively high intensity and duration. The short-circuit duration must be limited to the interval 0.9 – 1.5 s with a maximum current of 25 kA, although when requiring a higher short-circuit current between 25 - 45 kA, the test can last up to 5 s. It

is noted that according to this standard, the purpose of the short-circuit test is to reproduce only the thermal effects of the short-circuit current.

However, the results of the standard tests do not necessarily apply to all possible operating conditions, and specially to those conditions exceeding normal conditions of operations [22]. In this case the tests proposed in the standards are usually complemented by specific tests agreed between purchaser and supplier.

The transient current during the short-circuit test has a sinusoidal term with a superimposed DC component [10, 14, 23]. The target current to be achieved during the short-circuit test, also known as prospective short-circuit current, is as follows, [11]

$$i(t) = \sqrt{2} \cdot I_{RMS} \cdot \left[\sin(\omega \cdot t + \psi - \varphi) - \sin(\psi - \varphi) \cdot e^{-t \cdot (R/L)} \right] \qquad (1)$$

ω being the scalar angular frequency corresponding to the 50 Hz supply frequency, φ the phase angle of the impedance of the test loop which defines the power factor of the loop, and ψ the closing or initial phase angle of the voltage applied to the loop, measured at the precise instant of connection. It is worth noting that the exponential term (1) corresponds to the transient part, which can be modulated by a strict control of the $\psi - \varphi$ phase angle difference. For highly inductive circuits the phase angle of the loop impedance is $\varphi \approx \pi/2$ with $R << L$ and thus, the DC component presents a very slow decay. In the **short-time withstand current test** the initial phase of the voltage equals the phase angle of the loop impedance, that is, $\psi = \varphi$, so there is no DC component of the current since $\sin(\psi - \varphi) = 0$. Contrarily, the transient part is maximized when $\psi - \varphi = \pm \pi/2$. As a consequence, by controlling the initial phase angle ψ of the applied voltage at the precise instant of switching the circuit on, the transient part of the short-circuit current can be modulated.

Many electrical devices including power connectors are designed to withstand their assigned rated peak and short-time withstand currents with safety, i.e. without damaging the performance of the device. The IEC 62271-1 [8] defines the rated short-time withstand current I_k, as the root-mean-square value (RMS) of the current which the tested electrical equipment can carry during a specified time under recommended conditions. The rated peak withstand current I_p is defined as the peak or maximum value of the current waveform [10] which the electrical device to be tested can carry during a specified time under recommended conditions.

The rated duration of the short circuit t_k is defined as the time interval that the analyzed device can withstand the rated short-time withstand current, being its standard value 1 s, although other recommended values are 0.5 s, 2 s and 3 s [7]. Although the international standards do not prescribe a temperature limit to be reached during the short-time current withstand test [8, 24, 25], the temperature rise of the tested device

must ensure that no significant damage occurs.

The short circuit test has two main stages, that is, the heating and cooling phases. During the heating phase the short-time withstand current is typically applied for 1 s, and both the reference conductors and the connector suffer a sudden temperature rise. According to the IEC 61238-1 standard for mechanical connectors for power conductors [22], the short-circuit current must raise the temperature of reference conductors from an initial temperature below 35 °C to 250- 270 °C. Next, in the cooling phase, the test loop is disconnected from the mains, so the conductor tends to cool down. In this stage the connector is initially heated by the thermal influence of the reference conductors, which are much hotter, and after some time the connector slowly cools down to ambient temperature as shown in Fig. 2.
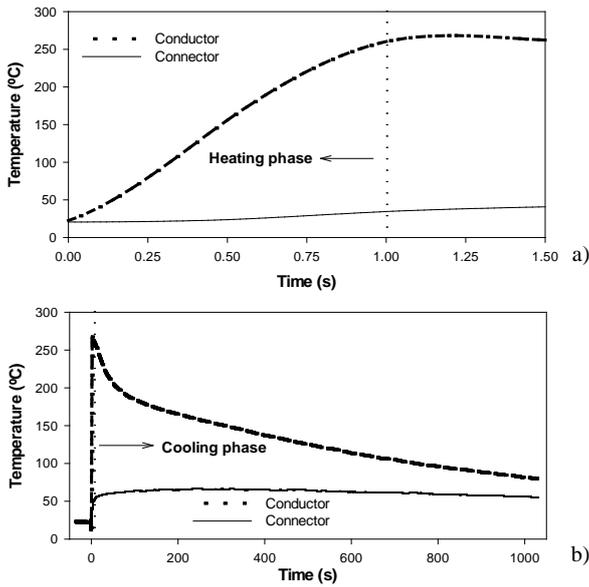

Fig. 2. Temperature evolution during the short-circuit test. a) Heating phase. b) Cooling phase.

4.   THE FDM APPROACH BASED ON A COUPLED ELECTROMAGNETIC-THERMAL MODEL

In the analyzed problem, Joule heating is by far the most important heat source. Due to the transient nature of the peak withstand current test, both the resistance R and the inductance L of the test loop, which includes the connectors and the conductors, can influence the thermal behavior during the short-circuit since L/R is the time-constant of the transient part of the current during the short-circuit. To accurately reproduce the coupled electro-thermal physics of the problem, conductive, convective and radiative effects will be considered during both the heating and cooling phases, although during the heating phase the process can be assumed as adiabatic [10] because the short-circuit is sufficiently short. This is a multiphysics problem, because electrical and thermal equations have to be solved simultaneously.

The method proposed here reduces the analyzed three-dimensional domain to a one-dimensional geometry which is discretized in small elements or nodes of the same length Δx. To determine the transient conditions

during the short-circuit test, the electro-thermal energy balance is calculated in each node, similarly as done in a previous research of the authors of this work [18] to simulate temperature rise tests. To increase accuracy and reduce drastically the computational burden, the one-dimensional model retains key information of the three-dimensional geometry from the CAD of the test object to determine the temperature distribution along the conductor and the connector. By this way different parameters related to the three-dimensional origin of each discrete node of the one-dimensional geometry are calculated. They include the outer perimeter and area, or the convective coefficient of each element.

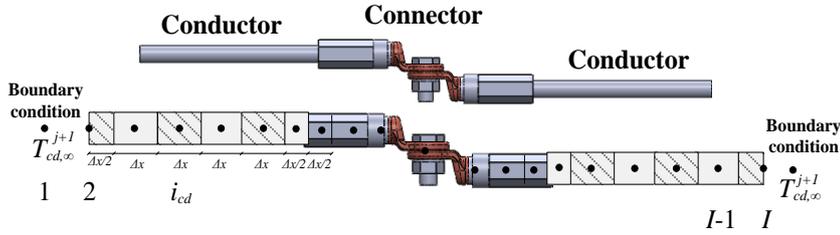Fig. 3 displays the reduction from a three-dimensional domain to one-dimension.

Fig. 3. Conductor-connector discretization.

The FDM approach calculates the temperature in each node based on the temperatures of the two adjacent right-side and left-side nodes. Since three nodal temperatures are involved at each calculation step, it results a three-term nodal temperature equation. The tri-diagonal matrix, defining the system of equations arising from the simultaneous solution of all nodes in the analyzed domain, can be solved by applying the tri-diagonal matrix algorithm (TDMA) [26]. The FDM formulation approximates the partial derivatives by means of the Taylor expansions in the discretized points of the analyzed system. The nodal temperatures are calculated from the temperature of the neighboring right-side and left-side nodes. The tri-diagonal equations system arising from this approach can be written as [18],

$$a_i^j \cdot T_{i-1}^{j+1} + b_i^j \cdot T_i^{j+1} + c_i^j \cdot T_{i+1}^{j+1} - d_i^j = 0 \qquad (2)$$

where i and j are the indices of the spatial and temporal steps, respectively, with $i = 1, 2, \ldots, I$ and $j = 1, 2, \ldots, J$. Therefore, $T_i^j = T(i \cdot \Delta x, j \cdot \Delta t)$ is the mean temperature of the i-th node calculated at the j-th time-step, being a_i^j, b_i^j, c_i^j and d_i^j constant coefficients. It is noted that Δx and Δt are, respectively, the discretized spatial and time steps considered in the simulations.

By assuming that coefficients a_i^j, b_i^j, c_i^j and d_i^j in (2) are known, the vector $[T_1^{j+1}, T_2^{j+1}, \ldots, T_I^{j+1}]$ of unknown nodal temperatures is obtained from the TDMA algorithm.

The coefficients a_i^j, b_i^j, c_i^j and d_i^j are calculated by applying the rate of energy balance equation in all nodes of the analyzed domain,

$$\dot{Q}_{change} = (\dot{Q}_{input} + \dot{Q}_{generation}) - (\dot{Q}_{output} + \dot{Q}_{consumption}) \qquad (3)$$

As depicted in Fig. 4, (3) can be rewritten as [10],

$$\dot{Q}_{change} = (\dot{Q}_{conduction\_left} + \dot{Q}_{generation}) - (\dot{Q}_{convection} + \dot{Q}_{radiation} + \dot{Q}_{conduction\_right}) \qquad (4)$$

being $\dot{Q}_{change}$ [W] the rate of energy change in the studied node or element, $\dot{Q}_{conduction\_left}$ the rate of energy

flowing into the left side wall of the node, $\dot{Q}_{generation}$ the rate of energy generated in the node and $\dot{Q}_{conduction\_right}$

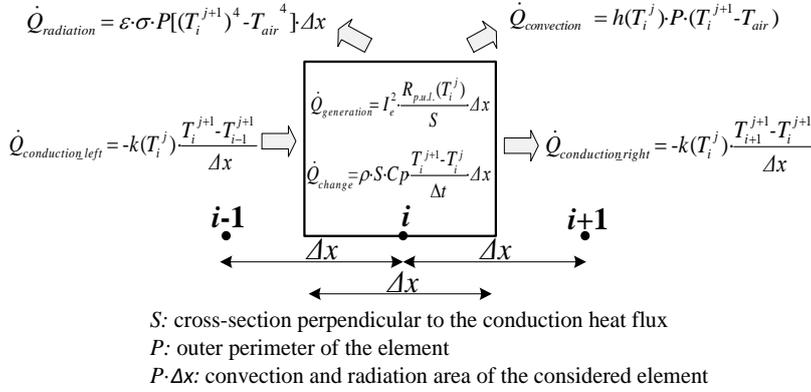the rate of energy flowing away from the right wall of the node under analysis.

S: cross-section perpendicular to the conduction heat flux
P: outer perimeter of the element
P·Δx: convection and radiation area of the considered element

Fig. 4. Rate of energy balance in a general element of the studied domain.

It is noted that parameters *S, h* and *P* are calculated in each element along the domain since they depend on the three-dimensional geometry of the problem.

The generation term requires knowledge of the electrical resistance of each nodal element. The resistance of the conductor is obtained from the manufacturer datasheet, which is usually provided at 20 ºC in Ω/km. Due to its complex geometry, the resistance of the connector is calculated from its CAD model. The connector geometry is divided in several parts or slices of the same thickness, their parallel faces being perpendicular to the electrical current flow. The envelope of each part and the inner cross section within this envelope is determined by means of a convex-hull algorithm, from which the resistance of the connector is calculated as the addition of the incremental resistances of all slices.

To set the initial conditions, it is assumed that the tested objects have been acclimated in the test room, so they have the same initial temperature than the temperature of the surrounding air $T_{air,\infty}$,

$$T_i^{j=1} = T_{air,\infty} \qquad i = 1,...,I \qquad (6)$$

Regarding the boundary conditions, the convective and radiative cooling effects have been considered in all nodes of the analyzed domain, respectively, as,

$$\dot{Q}_{convection} = h(T_i^j) \cdot P \cdot (T_i^{j+1} - T_{air}) \cdot \Delta x \qquad (8)$$

$$\dot{Q}_{radiation} = \varepsilon \cdot \sigma \cdot P[(T_i^{j+1})^4 - (T_{air}^{j+1})^4] \Delta x \qquad (9)$$

The h coefficient of both the conductors and the connector is computed from the dimensionless Nusselt number Nu, the thermal conductivity k [W/(m·K)] of atmospheric air and the characteristic length L_c [m],

$$h(T_i^j) = k \cdot Nu / L_c \qquad (7)$$

The characteristic length of the conductor is its diameter and the characteristic length of the connector is the cubic root its volume [27].

The convective coefficient $h_{conductor}$ of the conductor was calculated from the Nusselt number from Churchill & Chu for horizontal cylinders with natural convection [28]. The convective coefficient of the connector $h_{connector}$ was calculated from the Nusselt number of Qureshi and Ahmad [29, 30] for natural convection in horizontal cylinders. To this end, the 3D geometry of the connector is considered since the weighted average value $h_{connector}$ was calculated by considering the angular orientation of each of the individual triangular faces of the surface mesh of the connector, which is directly generated by the CAD software. Since the Nusselt number depends on the temperature, it was reevaluated at each time-step.

5. EXPERIMENTAL SETUP

To validate the simulation method proposed in this work, experimental short-circuit tests were conducted in the AMBER laboratory of the Universitat Politècnica de Catalunya and performed based in the IEC 61238-1/2003 standard [22].

The experimental setup includes a 120 kVA bi-phase variable autotransformer [0V-400V] connected to a 120 kVA 400/10 V transformer whose rated output values are 0-10 V, 0-10 kA. The output of this transformer was connected to the test loop. The loop current was measured with a calibrated Fluke i6000s-Flex Rogowski coil with an uncertainty of 2%.

The test loop, which is shown in Fig. 5, was composed of three sections of AAC conductor (AL-XZ1 1x120K from Prysmian) of 1.5 m each and outer diameter $D_{cd} = 13.0$ mm and six bimetallic YAT120AM130CP compression connectors for low- and medium-voltage applications.
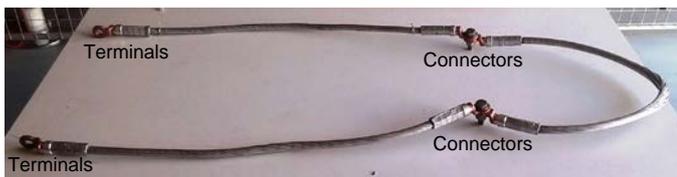

Fig. 5. AL-XZ1 1x120K conductor loop used during the short-circuit test.

Temperature measurements were performed by means of three T-type PFA-exposed welded-tip thermocouples (temperature range from -75ºC to +250ºC) with a diameter of 0.2 mm and Teflon™ PFA

cover which were placed on the second layer of strands of the tested conductor. Thermocouples signals were acquired every 14 ms by means of an OMEGA DAQ USB-2400 acquisition card.

Experimental tests were performed under atmospheric conditions (11 ºC, 982.7 hPa and 52.3% relative humidity). A short-circuit current of $I_{RMS} = 8650$ A_{RMS} that decreases until 7200 A_{RMS} due to the increase of the test loop resistance caused by the temperature rise, was applied during 3 seconds.

6. RESULTS AND MODEL VALIDATION

This section summarized the results obtained with the FDM simulation approach which are compared against experimental results obtained by using the experimental setup described in Section V. In addition, results from 3D-FEM simulations were conducted to illustrate the accuracy of the FDM-based approach.

Tables 1 and 2 summarize the values of the physical properties considered in the simulations.

Table 1 Physical properties of the conductor at 20ºC

Variable	Value
Conductor designation	AL-XZ1 1x120K
Conductor type	AAC
Conductor diameter	13.0 mm
Aluminum alloy	AA-6101
Mass of the conductor	420 kg/km
Thermal heat capacity of aluminum, Cp_{Al}	900 J/(m·K)
Thermal conductivity of aluminum, kp_{Al}	209 W/(m·K)
Electrical resistance of the conductor, $R_{,20ºC}$	0.238 Ω/km
Temperature coefficient , α_{cd}	0.004 1/K
Emissivity of aluminum ε	0.5

Table 2 Physical properties of the connector at 20ºC

Variable	Value
Connector designation	YAT120AM130CP
Connector type	Cu-Al compression
Aluminum alloy	EN AW-1050A
Aluminum density	2700 kg/m³
Electrical resistivity of aluminum alloy, ρ_{Al}	6.74·10⁻⁸ Ω·m
Temperature coefficient of aluminum, α_{Al}	0.004 1/K
Thermal heat capacity of aluminum, Cp_{Al}	900 J/(kg·K)
Thermal conductivity of aluminum, kp_{Al}	209 W/(m·K)
Copper alloy	Cu-ETP
Copper density	8960 kg/m³
Electrical resistivity of copper, ρ_{Al}	1.71·10⁻⁸ Ω·m
Thermal heat capacity of copper, Cp_{Cu}	390 J/(kg·K)
Thermal conductivity of copper, kp_{Cu}	400 W/(m·K)
Temperature coefficient of copper, α_{Cu}	0.004 1/K
Emissivity of the connector, ε	0.5
Stainless steel (bolting elements)	A304
Electrical resistivity of steel, ρ_{steel}	72·10⁻⁸ Ω·m
Thermal heat capacity of steel, Cp_{steel}	490 J/(kg·K)
Thermal conductivity of steel, kp_{steel}	15 W/(m·K)
Temperature coefficient of steel, α_{steel}	0.0024 1/K

Table 3 shows the time-step and the spatial-steps considered in the simulations performed as well as the duration of the simulations.

Table 3 Calculation parameters of the simulation

Variable	Value
Time-step during the short-circuit (Δt)	0.4 ms
Time-step during the cooling stage (Δt)	1 s
Short-circuit duration	3 s
Simulation time	1000 s
Spatial-step (Δx)	1 mm

Fig. 6 shows the experimental profile of the short-circuit current, which is used as input of the simulation method proposed in this work. Note the negative peak during the first current cycle due to the transient.
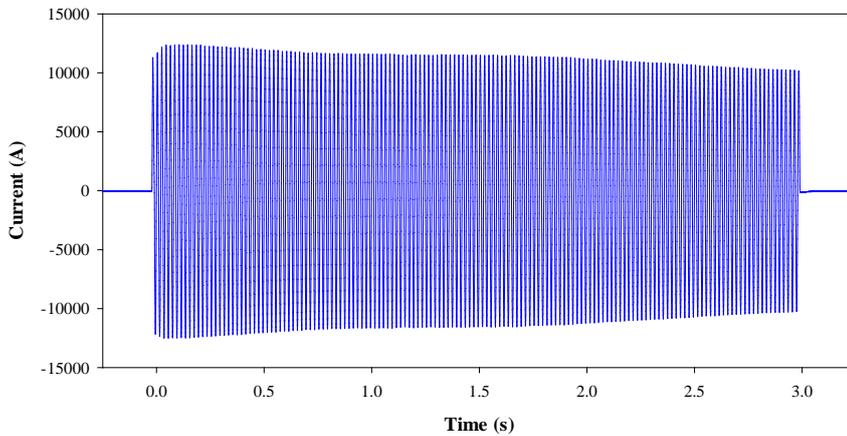

Fig. 6. Experimental current during the short-circuit test.

The amplitude reduction of the current shown in Fig. 6 is consequence of the resistance increase due to the heating effect of the short-circuit, since a constant voltage amplitude was applied.

Fig. 7a shows the evolution of the temperature measured in the laboratory as well as the temperature evolution predicted by the simulation model proposed in this work and the curve obtained by means of 3D-FEM simulations according to [14] using a variable time-step with an average value of 0.4 ms. It is shown that both FEM and the FDM-based approaches provide almost the same results during both the heating and cooling phases.
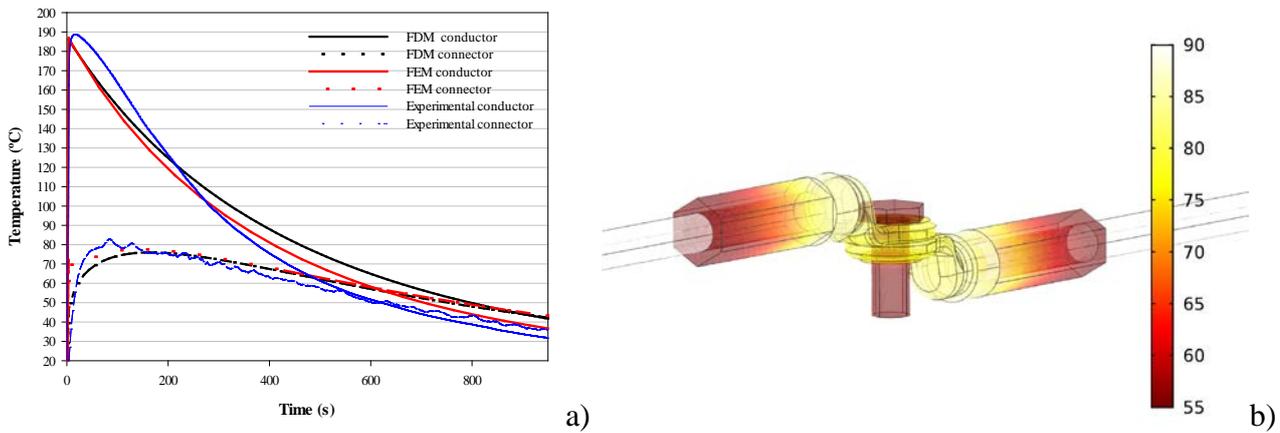
Fig. 7. Short-circuit test. a) Comparison between the experimental temperature (°C) obtained during the test and the temperature obtained by means of the FDM and FEM approaches. b) Temperature profile of the YAT120AM130CP connector including the bolting elements, obtained by means of 3D-FEM just at the end of the short-circuit ($t = 3$ s).

Table 4 summarizes the average differences between experimental data and simulation results.

Table 4 Average difference with respect to measured data

Element	FDM	FEM
Conductor	3.11%	1.86%
Connector	1.52%	1.80%

Fig. 8a shows both the instantaneous and average heating (Joule) power in the conductor calculated by means of the simulation model. Fig. 8a also shows that the power generated by the Joule effect is zero during the cooling phase of the short-circuit test ($t > 3$ s). Fig. 8b displays the cooling power due to the radiative and convective effects. It is worth noting that one can assume an adiabatic behavior during the short-circuit test due to the large difference between the heat generated and evacuated by convection and radiation phenomena.
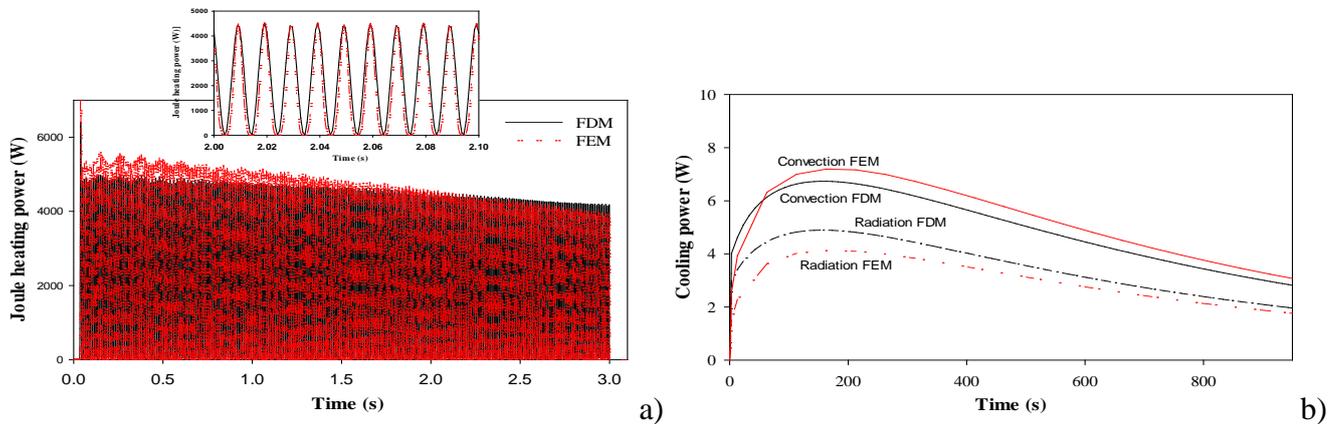

Fig. 8. a) Instantaneous power generated due to the Joule effect during the short-circuit interval. b) Convective and radiative cooling power evacuated through the surface of the connector.

Fig. 8b also shows that the use of two different models of convection for the FDM simulation and the FEM simulation leads to small differences of the final result of cooling power. These are also caused by the differences in the final temperature reached at the end of the short-circuit and due to the heterogeneity of temperature values along the connector surface.

The elapsed time to run a complete simulation with the FDM simulation tool, considering a time-step of 0.4 ms, is less than 1 h using a 2x2.27 GHz Intel® Xeon® CPU with 24 GB RAM. The 3D-FEM simulation time by considering the same time-step is of about 48 h, and 2h with a time-step of 0.33 s.

7. CONCLUSION

Standard short-circuit tests are compulsory for many electrical hardware including power connectors. These tests must be performed in high-power laboratories with short-circuit capability, which due to the enormous power requirements, investment and maintenance costs are beyond the reach of many small and medium companies. Therefore these tests are often externalized to some scarce and singular high-power laboratories. This results in manufacturing delays and cost increases due the high price and the long waiting times of such tests. To ensure that the connectors fulfill the requirements of such tests and thus reducing them to the minimum, an improved thermal design is mandatory. Therefore it is essential to dispose of fast and accurate simulation tools to determine the temperature achieved by the connector and the reference conductors during both the heating and cooling phases of the short-circuit. This paper has proposed a fast and accurate FDM method, based on one-dimensional reduction, to simulate the thermal behavior of both the conductors and connectors during the short-circuit test. It has been proved that the proposed approach can accurately predict in a fast manner the temperature rise of both the conductor and the connector during short-circuits as well as the cooling stage once the short-circuit current has been cleared. The contribution of the proposed model can be significant, since it can be applied to other components of power lines and substations, and it can assist the optimal design stage of connectors and other hardware in a fast and simple manner. By this way it can be ensured that the connectors will adequately satisfy the requirements of the international standards in force.

BIBLIOGRAPHY

1   Wang, X., Ueda, H., Ishiyama, A., Ohya, M., Yumura, H., Fujiwara, N.: 'Numerical simulation on fault current condition in 66kV class RE-123 superconducting cable'*Phys. C Supercond.*, 2010, **470**, (20), pp. 1580–1583.

2   Sousa, W.T.B. d., Polasek, A., Dias, R., *et al.*: 'Short-Circuit Tests and Simulations with a SCFCL Modular Assembly'*Phys. Procedia*, 2012, **36**, pp. 1242–1247.

3   Li, H., Bose, A., Zhang, Y.: 'On-line short-circuit current analysis and preventive control to extend equipment life'*IET Gener. Transm. Distrib.*, 2013, **7**, (1), pp. 69–75.

4   Filippakou, M.P., Karagiannopoulos, C.G., Agoris, D.P., Bourkas, P.D.: 'Electrical contact overheating under short-circuit currents'*Electr. Power Syst. Res.*, 2001, **57**, (2), pp. 141–147.

5   Fan, Y., Wen, X., Jafri, S.A.K.S.: '3D transient temperature field analysis of the stator of a hydro-generator under the sudden short-circuit condition'*IET Electr. Power Appl.*, 2012, **6**, (3), p. 143.

6   Chen, T.-H., Liao, R.-N.: 'Modelling, simulation, and verification for detailed short-circuit analysis of a 1×25 kV railway traction system'*IET Gener. Transm. Distrib.*, 2016, **10**, (5), pp. 1124–1135.

7   International Electrotechnical Commission: 'IEC-60694. Common specifications for high-voltage switchgear and controlgear standards' (1996), p. 179

8   International Electrotechnical Commission: 'IEC 62271-1:2007. High-voltage switchgear and controlgear - Part 1: Common specifications' (International Electrotechnical Commission, 2007), p. 252

9   'ANSI C37.51a-2010 Switchgear - Metal-Enclosed Low-Voltage AC Power Circuit Breaker Switchgear Assemblies -Conformance Test Procedures', http://webstore.ansi.org/RecordDetail.aspx?sku=ANSI+C37.51a-2010, accessed October 2015

10   Polykrati, A.D., Karagiannopoulos, C.G., Bourkas, P.D.: 'Thermal effect on electric power network components under short-circuit currents'*Electr. Power Syst. Res.*, 2004, **72**, (3), pp. 261–267.

11   Li, X., Qu, J., Wang, Q., Zhao, H., Chen, D.: 'Numerical and Experimental Study of the Short-Time Withstand Current Capability for Air Circuit Breaker'*IEEE Trans. Power Deliv.*, 2013, **28**, (4), pp. 2610–2615.

12   Hamzeh, M., Sheshyekani, K., Kadkhodaei, G.: 'Coupled electric–magnetic–thermal–mechanical modelling of busbars under short-circuit conditions'*IET Gener. Transm. Distrib.*, 2016, **10**, (4), pp. 955–963.

13   Xiangyu Guan, Naiqiu Shu, Bing Kang, *et al.*: 'Multiphysics Analysis of Plug-In Connector Under Steady and Short Circuit Conditions'*IEEE Trans. Components, Packag. Manuf. Technol.*, 2015, **5**, (3), pp. 320–327.

14   Capelli, F., Riba, J.-R., Pérez, J.: 'Three-Dimensional Finite-Element Analysis of the Short-Time and Peak Withstand Current Tests in Substation Connectors'*Energies*, 2016, **9**, (6), p. 418.

15   Rezk, K., Forsberg, J.: 'A fast running numerical model based on the implementation of volume forces for prediction of pressure drop in a fin tube heat exchanger'*Appl. Math. Model.*, 2014, **38**, (24), pp. 5822–5835.

16   Wang, X., Jiang, Y.: 'Model reduction of discrete-time bilinear systems by a Laguerre expansion technique'*Appl. Math. Model.*, 2016.

17   Codecasa, L., dAlessandro, V., Magnani, A., Irace, A.: 'Circuit-Based Electrothermal Simulation of Power Devices by an Ultrafast Nonlinear MOR Approach'*IEEE Trans. Power Electron.*, 2016, **31**, (8), pp. 5906–5916.

18   Abomailek, C., Capelli, F., Riba, J.-R., Casals-Torrens, P.: 'Transient thermal modelling of substation connectors by means of dimensionality reduction'*Appl. Therm. Eng.*, 2017, **111**, pp. 562–572.

19   Chvala, A., Donoval, D., Marek, J., Pribytny, P., Molnar, M., Mikolasek, M.: 'Fast 3-D Electrothermal Device/Circuit Simulation of Power Superjunction MOSFET Based on SDevice and

HSPICE Interaction'*IEEE Trans. Electron Devices*, 2014, **61**, (4), pp. 1116–1122.

20   AENOR: 'UNE-EN 573-3:2014. Aluminium and aluminium alloys - Chemical composition and form of wrought products - Part 3: Chemical composition and form of products' (AENOR, 2014), p. 36

21   AENOR: 'UNE-EN 13601:2014. Copper and copper alloys - Copper rod, bar and wire for general electrical purposes' (AENOR, 2014), p. 30

22   International Electrotechnical Commission: 'IEC 61238-1:2003. Compression and mechanical connectors for power cables for rated voltages up to 30 kV (Um = 36 kV) - Part 1: Test methods and requirements' (2003), p. 115

23   Tartaglia, M., Mitolo, M.: 'Evaluation of the Prospective Joule Integral to Assess the Limit Short Circuit Capability of Cables and Busways', in '2008 IEEE Industry Applications Society Annual Meeting' (IEEE, 2008), pp. 1–5

24   IEEE: 'IEEE Std C37.20.1-2015 (Revision of IEEE Std C37.20.1-2002). IEEE Standard for Metal-Enclosed Low-Voltage (1000 Vac and below, 3200 Vdc and below) Power Circuit Breaker Switchgear' (IEEE, 2015), pp. 1–84

25   IEEE: 'IEEE Std C37.13.1-2006. IEEE Standard for Definite-Purpose Switching Devices for Use in Metal-Enclosed Low-Voltage Power Circuit Breaker Switchgear' (IEEE, 2006), pp. c1-18

26   Datta, B.N.: 'Numerical Linear Algebra and Applications, Second Edition' (SIAM, 2010, Second edi)

27   J.Oliver, M. Cervera, S. Oller, J.L.: 'Isotropic damage models and smeared crack analysis of concrete'*Proc. SCI-C Comput. Aided Anal. Des. Concr. Struct.*, 1990, **945958**.

28   Churchill, S.W., Chu, H.H.S.: 'Correlating equations for laminar and turbulent free convection from a horizontal cylinder'*Int. J. Heat Mass Transf.*, 1975, **18**, (9), pp. 1049–1053.

29   Boetcher, S.: 'Natural Convection from Circular Cylinders' (Springer, 2014)

30   Qureshi, Z.H., Ahmad, R.: 'Natural convection from a uniform heat flux horizontal cylinder at moderate rayleigh numbers',*Numer. Heat Transf.*, 1987, **11**, (2), pp. 199–212.